Theoretical analysis of earth pressure against rigid retaining walls under translation mode

AUTHOR(S):

Khosravi, Mohammad Hossein; Pipatpongsa, Thirapong; Takemura, Jiro

Soils and Foundations 2016;56(4):664–675

HOSTED BY

ELSEVIER

The Japanese Geotechnical Society

Soils and Foundations

www.sciencedirect.com
journal homepage: www.elsevier.com/locate/sandf

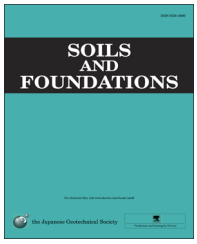

Technical Paper

Theoretical analysis of earth pressure against rigid retaining walls under translation mode

Mohammad Hossein Khosravi[a,*], Thirapong Pipatpongsa[b], Jiro Takemura[c]

[a]School of Mining Engineering, College of Engineering, University of Tehran, Iran
[b]Department of Urban Management, Kyoto University, Japan
[c]Department of Civil and Environmental Engineering, Tokyo Institute of Technology, Japan

Received 5 May 2015; received in revised form 17 November 2015; accepted 30 March 2016
Available online 30 July 2016

Abstract

The soil mass behind a retaining wall gradually yields and separates from the stationary soil mass with the complex shape of the slip surface depending on the mode of wall movement and roughness of the wall surface. In this study, the problem of a rigid retaining wall with a uniform surcharge acting along the horizontal backfill under active translation mode is investigated in a two-dimensional system of equilibrium. Exact stress solutions based on Janssen's approach are generalized in rectangular coordinates and are validated with boundary conditions on the retaining wall and at the Coulomb slip line behind the wall. Because the yield condition is not used in Janssen's approach, the proposed solution is a merely static stress solution, not statically admissible solution. New equations are developed to estimate the magnitude and distribution of vertical, horizontal and shear stresses in the failure zone behind a retaining wall. The proposed analysis indicates the arching effect behind the retaining wall because the maximum stresses do not appeared at the toe; but at some distance away from the toe of the retaining wall. The results of the proposed formulations are compared with both full-scale and laboratory-scale experimental data as well as the existing formulations. The proposed analysis provides comparable approximations for horizontal active stress distribution, the magnitude and the application height of the horizontal active force at the wall.

Keywords: Retaining walls; Soil/structure interaction; Arching effect; Earth pressure; Stress analysis; Failure

1. Introduction

Conventionally, the active earth pressure against rigid retaining walls has been calculated by using Coulomb (1776) or Rankine (1857) formulation with a consequence of linear distribution of active earth pressure against the wall. However, many experimental results (Tsagareli, 1965; Sherif and Fang, 1984; Fang and Ishibashi, 1986; Chang, 1997; Take and Valsangkar, 2001; O'Neal and Hagerty, 2011) show that the distribution of active earth pressure on a wall is non-linear for rough walls. According to Iskander et al. (2013), this non-linearity depends on the mode of wall movement and soil-wall friction angle.

The arching theory is attributed to Janssen (1895) with his observation of non-hydrostatic pressure in granular material stored in silos (Sperl, 2006). A differential equation for pressures in silos was formulated using force equilibrium along the direction of gravity under the assumption that the ratio of horizontal-to-vertical stress is constant. Janssen's stress solution in the form of an exponential function with depth provides the theoretical basis for arching effects in silos. More details relating to methods originating from the Janssen's

*Corresponding author.
Peer review under responsibility of The Japanese Geotechnical Society.

http://dx.doi.org/10.1016/j.sandf.2016.07.007

Nomenclature

The following symbols are used in this study:

x	horizontal distance measuring from the toe of the wall in a rectangular coordinate system
z	vertical distance measuring the from toe of the wall in a rectangular coordinate system
σ_1, σ_2, σ_3	major, intermediate and minor principal stresses
σ_x	horizontal stress
σ_z	vertical stress
τ_{xz}	shear stress
σ_{xw}	horizontal stress at the wall
σ_{zw}	vertical stress at the wall
τ_w	shear stress at the wall
α	angle between the slip surface and the wall measured from the vertical ($\alpha=\pi/4-\phi/2$)
ρ	bulk density of the retained soil
γ	unit weight of the retained soil
ϕ	internal friction angle of the retained soil
δ	interface friction angle between the wall and the retained soil
μ_w	coefficient of wall friction ($\mu_w=\tan\delta$)
H	height of the retained soil
h	height measured from the top of the wall
h_a	height of application of the horizontal active force measured from the top of the wall
K_w	Krynine (1945)'s horizontal-to-vertical active stress ratio at the wall
K_a	Rankine (1857)'s active earth pressure coefficient
M	moment of the horizontal active stress about the wall base
n	constant number defined by $n=\mu_w K_w/\tan\alpha$
P_a	total active force on the wall
P_{ah}	horizontal active force normal to the wall
Q	uniform surcharge on the top surface of the retained soil
T	shearing force on the wall

concept can be found in Drescher (1991). Efforts have been made to extend Janssen's original one-dimensional description to two-dimensional descriptions in both rectangular and cylindrical coordinate systems using the additional assumption of uniform pressure across the horizontal plane which is equivalent to linear shear stress reduction from the wall (Jáky, 1948; Millet et al., 2006; Rahmoun et al., 2008; Rahmoun et al., 2009; Pipatpongsa and Heng, 2010).

Terzaghi (1943) found that the maximum earth pressure does not appear at the lower end of the wall but is located at a certain higher level. He used the term "arching in soils" and explained that soil arching is the ability of soil material to transfer shear stresses to a more stable portion. The concept of soil arching was experimentally realized using a trap door and a retaining wall. When a part of the support yielded, the soil on that part would tend to move toward the yielding support but the relative movement is resisted by the frictional resistance; hence, shear stress is transferred onto adjacent stationary parts.

Investigations of the silo effect have been extended to conical and wedge-shaped hoppers by Walker (1966) and Walters (1973). The width of the differential flat element is not constant like that of a silo problem but varies with depth. Later, Walters refined Walker's stress solution by considering the inclined shear stress acting along the edge of the differential flat element. The derived stress solutions in terms of a power function with depth provide the theoretical basis for arching effects in hoppers.

Later, many authors also described earth pressure distributions in terms of arching action (action (Marston and Anderson, 1913; Getzler et al., 1968; Wang and Yen, 1974). Handy and Spangler (2007) initially developed equations based on Janssen's arching theory to estimate the distribution of active horizontal stress against rigid retaining walls. The assumption of a wedge-shaped failure zone was employed in addition to the one-dimensional basic formulation of a silo. Later, several other researchers also attempted to apply the arching effect in the estimation of active earth pressures against rigid retaining walls (Handy, 1985; Harrop-Williams, 1989a, 1989b; Wang, 2000; Paik and Salgado, 2003; Goel and Patra, 2008; Nadukuru and Michalowski, 2012). Some of those researchers combined the basic formulation of stress in hoppers with a wedge-shaped failure zone assumption in retaining walls under horizontal translation mode and formulated a one-dimensional stress solution in the form of a power function with depth (Harrop-Williams, 1989b; Wang, 2000; Paik and Salgado, 2003; Goel and Patra, 2008). Nadukuru and Michalowski (2012) demonstrated arching in distribution of active load on retaining walls using discrete element method and differential slice method.

So far, all of those existing formulations have been investigated in a one-dimensional system of equilibrium by assuming a differential flat element between the wall and the Coulomb slip line behind the wall. Though these arching-based solutions were formulated in the bounds of the Coulomb wedge for a case of a smooth vertical wall and horizontal backfill, they are different from the classical Coulomb solution because not only the total force but the stress distribution along the wall are also obtained. The simplification of the formulations by averaging vertical pressure helps obtain the stress distribution only along the wall, but the stress distribution in the failure zone between the wall and the slip line still remains unclear.

Active earth pressure distribution under horizontal translation, rotation about the top, and rotation about the base are typical modes of movement for rigid retaining walls conventionally considered (Terzaghi, 1943). Fang and Ishibashi (1986) experimentally showed that, though the active wall displacement necessary to mobilize the active state at each depth of the wall is independent of types of wall movement, the pattern of horizontal pressure distribution along the wall

depends on the wall movement mode because each of which induces different variation in mobilization before reaching the limit state. Strong arching effect is observed for a wall rotating about the top while weak arching effect is observed for a wall undergoing translational movement.

Besides, outcomes of DEM analysis conducted by Nadukuru and Michalowski (2012) indicate that rotation modes of wall movement are associated with uneven mobilization of strength on the surface separating the moving backfill from the soil at rest. The velocity fields in the case of translation and rotation about the base tend to be parallel while those in the case of rotation about the top is more complicated. A rigid translation mode of the retaining wall is focused in the present study because the outward motion of the wall away from the backfill evenly induces the relative movements in a whole wedge of soil. Hence, a uniform shape of arch spreading from the wall to the slip surface can be reasonably assumed in the static stress analysis.

The proposed analysis takes account of the stress system only; not entering into the strain system because their governing equations are associated with static equilibrium of a rigid wedge-shaped body. Hence, the mechanisms of deformation of the soil at the grain scale are ignored. The aspects of the arching effect with reference to more recent works that delineate the mechanisms of deformation at the finer scale can be found in some literatures, e.g. shape of arch (Guo and Zhou, 2013), force chains (Guo, 2012), shear bands (Rechenmacher et al., 2011; Chupin et al., 2012).

In this study, the problem of a retaining wall under an active translation mode is investigated in a two-dimensional system of equilibrium. Analytic stress solutions in a rectangular coordinate system are derived by adopting the assumption of uniform vertical stress in any horizontal plane, which is the ideal condition previously used in two-dimensional silo problems.

As discussed in Pipatpongsa and Heng (2010) with regard to previous works on stress solutions to the silo problem, the assumption of a uniform vertical stress, assumed by Janssen (1895) is equivalent to the assumption of a linear reduction of shear stress assumed by Jáky (1948). It is unlikely that these conditions are essentially present in an arbitrary backfill of the retaining wall. Handy (1985) showed that the magnitude of the vertical stresses at a depth behind a retaining wall vary with the distance from the wall despite its average with respect to the major principal stress is varied in a narrow range between 0.94 and 0.95 for friction angles 10–40°.

Since the method of filling greatly affects the vertical pressure across the horizontal floor, the assumption of uniform vertical pressure in silos is over-simplified. According to Saul (1953) and Thay et al. (2012), the initial vertical pressure in the retained granular media is substantial uniform only when the air pluviation method or moving funnel with a constant dropping height is employed. Therefore, the result of this study is expected to work only for the types of backfill condition and preparation that meet the assumption of uniform vertical pressure.

Under this simplistic assumption, new solutions for vertical, horizontal and shear stresses are developed, which make it possible to estimate the magnitude of stresses at any arbitrary point in a failure zone, including along a retaining wall. To validate the accuracy of the developed equations, for the particular case of no surcharge on the retained soil and at the wall, comparison is made with existing experimental results (Tsagareli, 1965; Khosravi et al., 2013) as well as with the values calculated from equations proposed by other authors.

The results of this study could improve the knowledge of static earth pressures on rigid retaining walls under active translation mode, for a safer and more economical design of such structures.

2. Soil arching behind retaining walls

In this study, a rigid retaining wall is considered to be under a translating mode while retaining a granular backfill soil mass. The detailed analytical procedure for calculation of the active horizontal stresses applied on the wall under the arching effect is presented in this section.

The state of stress in the retained soil is considered based on Janssen's arching theory. If a mass of granular soil is retained between two parallel rigid vertical walls, it is assumed that the settlement of the retained soil stage is large enough to fully induce friction between the walls and the soil. Therefore, the weight of any differential flat element of soil can be partially supported by the frictional resistance at the walls.

Frictional resistance causes changes in the direction of the principal stresses acting on the differential element (Fig. 1(a)). Similarly, if a rigid retaining wall with a rough face moves away from the soil horizontally, the direction of the major and minor principal stresses on the differential flat element is changed due to the frictional resistance at the wall (Fig. 1(b)).

Coulomb's failure criterion, in which the slip surface determined from Mohr's stress circle and Coulomb's envelope is found to be a plane inclining at an angle of $\pi/4+\phi/2$ to the horizontals, is commonly used in practice. However, it is well known the slip surface that develops in the soil behind a rigid rough wall is curved rather than a plane. The Coulomb's envelope only holds when the wall is smooth where the soil-wall friction angle is zero. For a rough wall, the slip surface depends on the yielding mode of the wall and soil-wall friction angle.

Handy (1985) and Paik and Salgado (2003) employed this simplifying assumption to analyze the active earth pressure on a translating rigid wall in one dimension, considering the arching effects in the backfill. Along this plane, the axis of major principal stress σ_1 orients vertically and the axis of minor principal stress σ_3 orients horizontally, so the distance from the wall and this plane defines stacks of unsymmetrical arches as the trajectory of the minor principal stress. This distance changes with depth and becomes zero at the bottom of the wall (Fig. 1(b)).

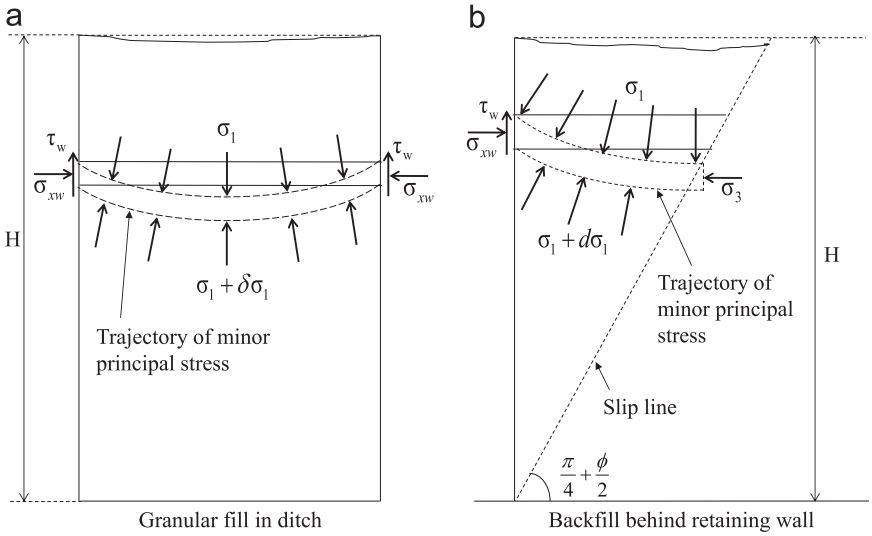

Fig. 1. Trajectory of minor principal stresses in granular materials (modified from Handy, 1985). (a) Granular fill in ditch. (b) Backfill behind retaining wall.

3. Proposed 2D analytical method

Referring to Fig. 1(b), Fig. 2 shows, with the reference axis, a free-body diagram of a differential element of backfill soil behind a retaining wall under translation mode with a uniform surcharge acting along the horizontal backfill. For a long retaining wall, the direction of intermediate principal stress σ_2 would be normal to the sectional plane shown in Fig. 2. Due to an assumption of plane strain condition, σ_2 is of no interest in this study; therefore, the problem can be reduced to two dimensions.

Sign conventions and notations in geo-mechanics are applied throughout this study where compression is taken as positive. The two-dimensional rectangular coordinate system (x, z) is placed at the corner of the failure wedge behind the retaining wall as shown in Fig. 2 where the z-axis is measured vertically upward passing the vertical face of the retaining wall and opposite to the direction of the gravity, while the x-axis is measured horizontally rightwards. The state of stress for a differential element of backfill soil illustrated in Fig. 2 must satisfy the two-dimensional equilibrium equations shown in Eqs. (1) and (2) where σ_x and σ_z are compressive stress components in horizontal and vertical directions, respectively, and τ_{xz} is a shear stress component.

$$\frac{\partial\sigma_x}{\partial x}+\frac{\partial\tau_{xz}}{\partial z}=0 \tag{1}$$

$$\frac{\partial\sigma_z}{\partial z}+\frac{\partial\tau_{zx}}{\partial x}=-\gamma \tag{2}$$

where γ is a bulk unit weight of granular material which is assumed constant throughout the whole body. In order to formulate a homogeneous partial differential equation, an additional partial differentiation with respect to x is taken to Eq. (2):

$$\frac{\partial^2\sigma_z}{\partial x\partial z}+\frac{\partial^2\tau_{xz}}{\partial x^2}=0. \tag{3}$$

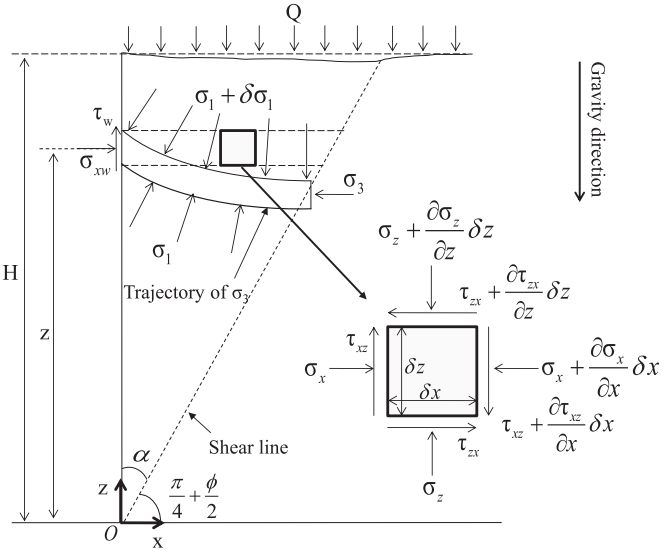

Fig. 2. Free-body stress diagram of a differential element of backfill soil behind a retaining wall under translation mode.

By imposing the assumption on uniformly distributed σ_z across the horizontal plane, in other words $\partial\sigma_z/\partial x=0$, Eq. (3) can be reduced to the following equation.

$$\frac{\partial^2\tau_{xz}}{\partial x^2}=0. \tag{4}$$

The general solution of Eq. (4) is given in Eq. (5) where c_1 and c_2 are functions of z due to integration of the partial differential equation:

$$\tau_{xz}=c_1(z)x+c_2(z). \tag{5}$$

Outward movement of the wall induces a small settlement of backfill soil; therefore, shear stress τ_w along the wall can be defined by substituting $x=0$ in Eq. (5), giving $\tau_{xz}(x,z)|_{x=0}=\tau_w(z)=c_2(z)$ as a function of z.

According to Harrop-Williams (1989a) as well as Paik and Salgado (2003), the trajectory of the minor principal stresses is defined as active arch transmitting a load from the wall and along its path to the slip surface where the failure wedge is isolated from the stationary soil mass. Due to the practical assumption of a slip surface behind a retaining wall with slope angle $\alpha=\pi/4-\phi/2$ measured from the verticals and a rotation of principal stresses as shown in Fig. 2, the minor principal stress must be horizontal at the right edge of the soil wedge. It follows that the vertical shear has its maximum value on the wall and gradually vanishes on the principal plane where the minor principal direction is aligned horizontally at the slip surface. Therefore, the vertical shear stress is zero on the vertical plane at the right edge of the soil wedge because the vertical plane on the slip line is the direction of the major principal axis, implying $\tau_{xz}(x,z)|_{x=z\tan(\alpha)}=0$. Note that shear stress on the slip surface is not zero but stays in equilibrium with self-weight and principal stresses along the slip surface; therefore, its magnitude can be determined later once the solutions of stress field are known.

To satisfy both boundary conditions of shear stress at $x=0$ and $x=z\tan(\alpha)$, Eq. (5) reveals that $c_1(z)=-\tau_w(z)/z\tan(\alpha)$ and $c_2(z)=\tau_w(z)$. Therefore, $\tau_{xz}(x,z)$ is formulated into the following equation, using Eq. (5):

$$\tau_{xz}(x,z)=\left(1-\frac{x}{z\ \tan\ \alpha}\right)\tau_w(z) \tag{6}$$

The expression of $\tau_{xz}(x,z)$ indicates that the shear stress acting along a horizontal plane is linearly reduced with the horizontal distance from the wall. This result is identical to the assumption of shear stress reduction introduced by Jáky (1948) in his formulation of stress distribution in silos. The limiting stress under active wall movement suggests that τ_w is mobilized and can be expressed by Eq. (7) in terms of $\sigma_{xw}(z)=\sigma_x(x,z)|_{x=0}$ which is an active horizontal stress at the wall at a given depth z:

$$\tau_w(z)=\mu_w\sigma_{xw}(z) \tag{7}$$

Janssen (1895) considered the state of stress of the material adjacent to the wall using a constant ratio $K_w=\sigma_{xw}(z)/\sigma_{zw}(z)$.

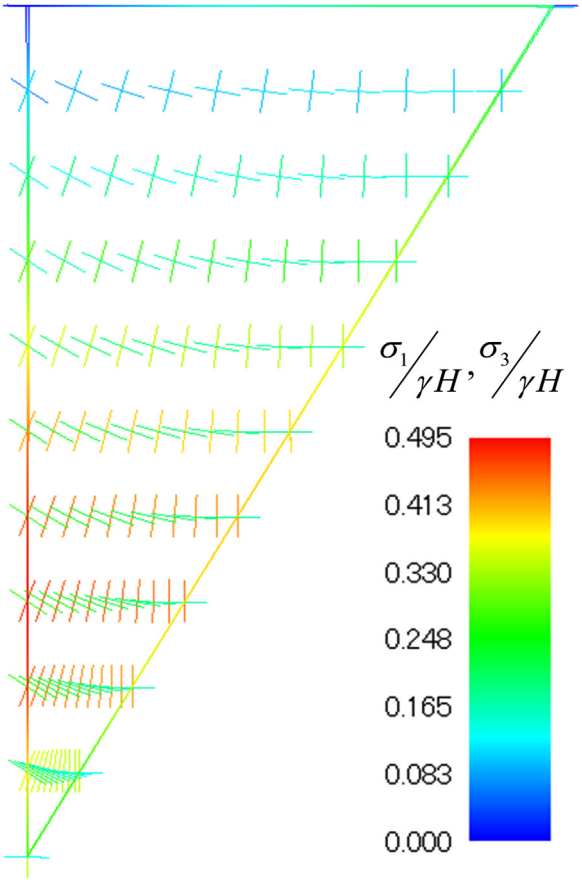

Fig. 4. Principal stresses in the failure wedge behind a fully rough retaining wall under active translation mode ($\phi=\delta=35^o$, $Q=0$).

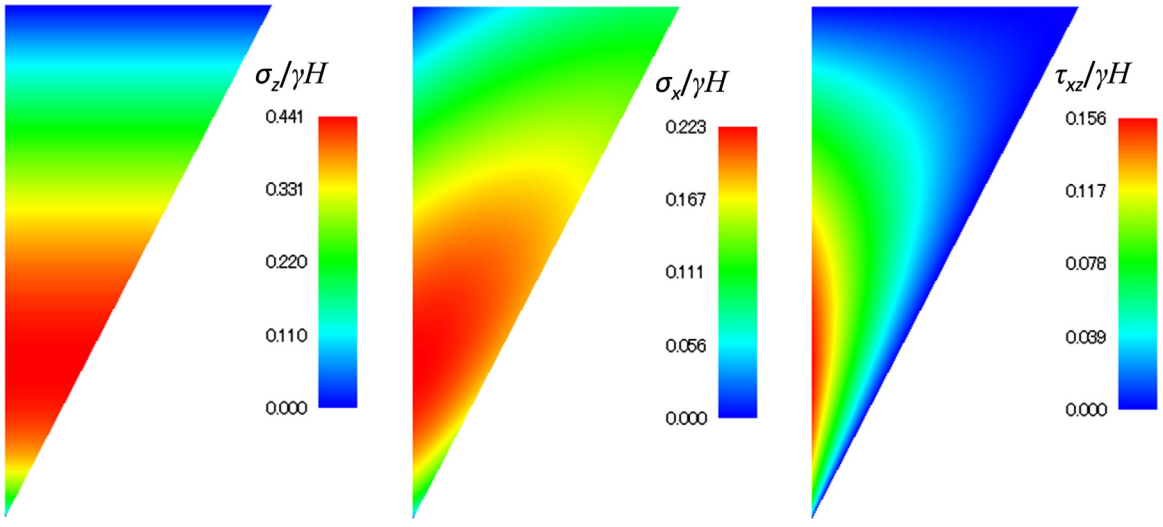

Fig. 3. Contours of normalized vertical, horizontal and shear stresses in the failure wedge behind a fully rough retaining wall under active translation mode ($\phi=\delta=35^o$, $Q=0$).

Herein, $\sigma_{zw}(z)$ is a vertical stress evaluated at the wall. Due to the assumption on uniformly distributed σ_z across the horizontal plane, therefore, $\sigma_{zw}(z)=\sigma_z(z)$ and active horizontal stress $\sigma_{xw}(z)$ with the magnitude less than $\sigma_{zw}(z)$ in a case of active condition is expressed in Eq. (8). According to Krynine (1945) and Walker (1966), this equation suggests that the state of stress adjacent to the wall yields simultaneously with the shear mobilization along the wall.

$$\sigma_{xw}(z)=K_w\sigma_z(z) \tag{8}$$

$$K_w=\frac{1-\cos\left(\sin^{-1}\left(\frac{\sin\delta}{\sin\phi}\right)-\delta\right)\sin\phi}{1+\cos\left(\sin^{-1}\left(\frac{\sin\delta}{\sin\phi}\right)-\delta\right)\sin\phi} \tag{9}$$

where K_w is the horizontal-to-vertical active stress ratio at the wall, δ is a frictional angle between the wall and granular media, and ϕ is the internal frictional angle of granular media in which $\delta\le\phi$.

Eq. (6) can be rewritten in the following form after substitutions of Eqs. (7) and (8) into it:

$$\tau_{xz}(x,z)=\left(1-\frac{x}{z\tan\alpha}\right)\mu_w K_w\sigma_z(z) \tag{10}$$

where $\mu_w=\tan\delta$ is a static coefficient of friction between the granular material and the wall.

Eq. (2) substituted by Eq. (10) can be arranged to obtain $\partial\sigma_z/\partial z$ which is a function of z; therefore $\partial\sigma_z/\partial z$ is replaced by $d\sigma_z/dz$. Consequently, the following linear non-homogeneous

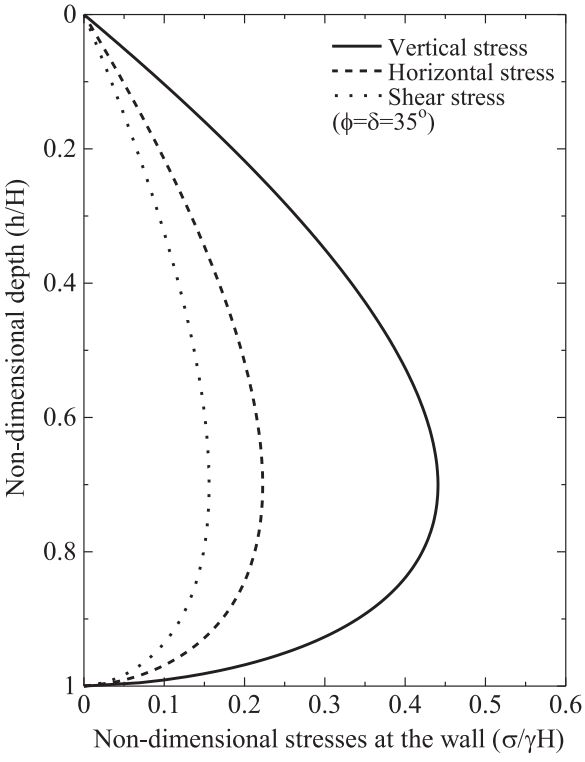

Fig. 5. Distribution of vertical, horizontal and shear stresses at a retaining wall under active translation mode ($\phi=\delta=35^o$, $Q=0$).

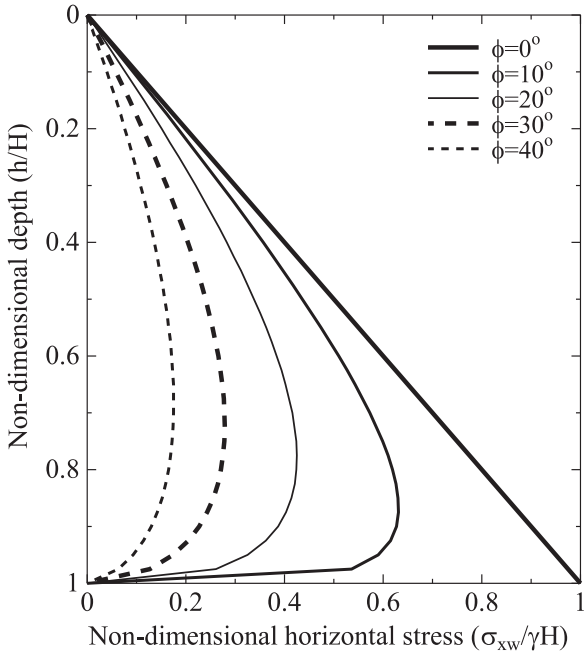

Fig. 6. The influences of soil internal friction angle on the active earth pressure ($\phi=\delta$, $Q=0$).

first-order differential equation can be formulated:

$$\frac{d\sigma_z(z)}{dz}-n\frac{\sigma_z(z)}{z}=-\gamma \tag{11}$$

where a constant $n=\mu_w K_w/\tan\alpha$ is introduced.

Integrating factor z^{-n} is multiplied on both sides in order to rearrange Eq. (11) into a solvable form:

$$\frac{d}{dz}(z^{-n}\sigma_z(z))=-\gamma z^{-n} \tag{12}$$

A general solution of Eq. (12) consists of two conditions for $n=1$ for a special case or else for a general case. The solution for a special case is obtained by substituting $n=1$ to Eq. (12) and is rearranged into a linear first order equation:

$$\sigma_z(z)=\begin{cases} c_3 z-\gamma z\ln(z) & \text{if } n=1 \\ c_4 z^n+\frac{\gamma z}{n-1} & \text{otherwise} \end{cases} \tag{13}$$

where c_3 and c_4 are integration constants.

The special case $n=1$ represents the case of a fully rough wall with $\phi=\delta=90^\circ$; therefore, this case is not realizable in reality. Accordingly, the special case is dropped and a solution for the general case is considered as the latter part of Eq. (13).

Applying the boundary condition at the ground surface behind the wall where a uniform surcharge Q is applied at the top surface of the backfill, $\sigma_z|_{z=H}=Q$ to obtain c_4:

$$c_4=\frac{Q}{H^n}-\frac{\gamma}{(n-1)H^{n-1}} \tag{14}$$

Substitution of Eq. (14) into the latter part of Eq. (13) obtains the vertical stress at the wall at a given height z:

$$\sigma_z(z)=\frac{\gamma H}{1-n}\left[\left(\frac{z}{H}\right)^n-\frac{z}{H}\right]+Q\left(\frac{z}{H}\right)^n. \tag{15}$$

Substitution of Eq. (15) into Eq. (10) obtains τ_{xz} at any arbitrary point (x, z) behind the wall:

$$\tau_{xz}(x,z) = n\left(\tan\alpha - \frac{x}{z}\right)\sigma_z(z). \tag{16}$$

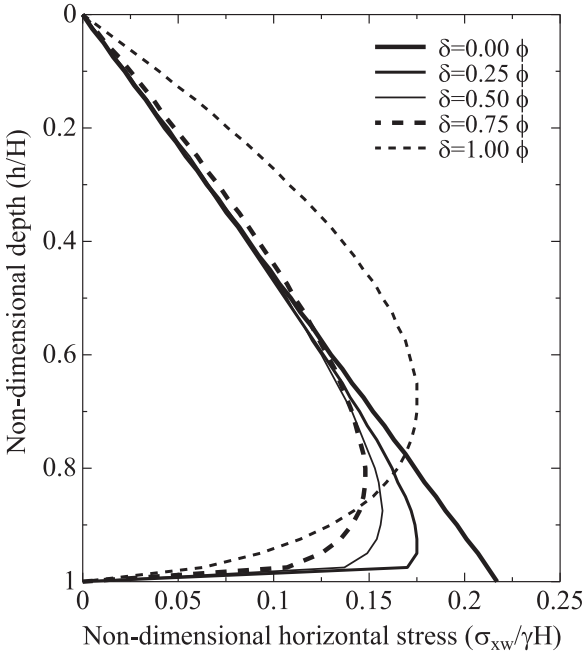

Fig. 7. The influences of wall-soil interface friction angle on the active earth pressure ($\phi=35^o$, $Q=0$).

Finally, the horizontal stress behind the retaining wall can be derived from Eq. (1) by integrating the differential equation from a wall to an arbitrary distance x. Note that all derivations are limited to the failure wedge with $x \le z\tan\alpha$ for a given z:

$$\sigma_x(x,z) = -\int_0^x \frac{\partial\tau_{xz}(x,z)}{\partial z}dx + K_w\sigma_z(z) \tag{17}$$

where $\sigma_x(x,z)|_{x=0} = \sigma_{xw}(z) = K_w\sigma_z(z)$.

Note that according to Handy (1985), the horizontal-to-vertical active stress ratio at the wall, K_w, is calculated from the equation developed by Krynine (1945) as shown in Eq. (9). For a fully smooth wall where the interface friction angle between the wall and the retained soil, δ, is zero, K_w reduces to Rankine's active earth pressure coefficient, K_a. Still, K_w is different from Coulomb's active earth pressure that includes the effect of δ. Therefore, comparison with other solutions when $\delta > 0$ should pay close attention to the dissimilar definitions of these coefficients.

Substitution of Eqs. (15) and (16) into Eq. (17) obtains the horizontal stress at distance x and height z behind the wall:

$$\sigma_x(x,z) = \left(K_w - n^2\tan\alpha\frac{x}{z} + \frac{(n-1)n}{2}\left(\frac{x}{z}\right)^2\right)\sigma_z(z) + \frac{n\gamma x}{2}\left(2\tan\alpha - \frac{x}{z}\right). \tag{18}$$

For the case of zero surcharge $Q=0$, despite σ_z and τ_{xz}, satisfies zero traction along the top layer where $z=H$, σ_x does not vanish to zero, resulting in a pre-compressed horizontal

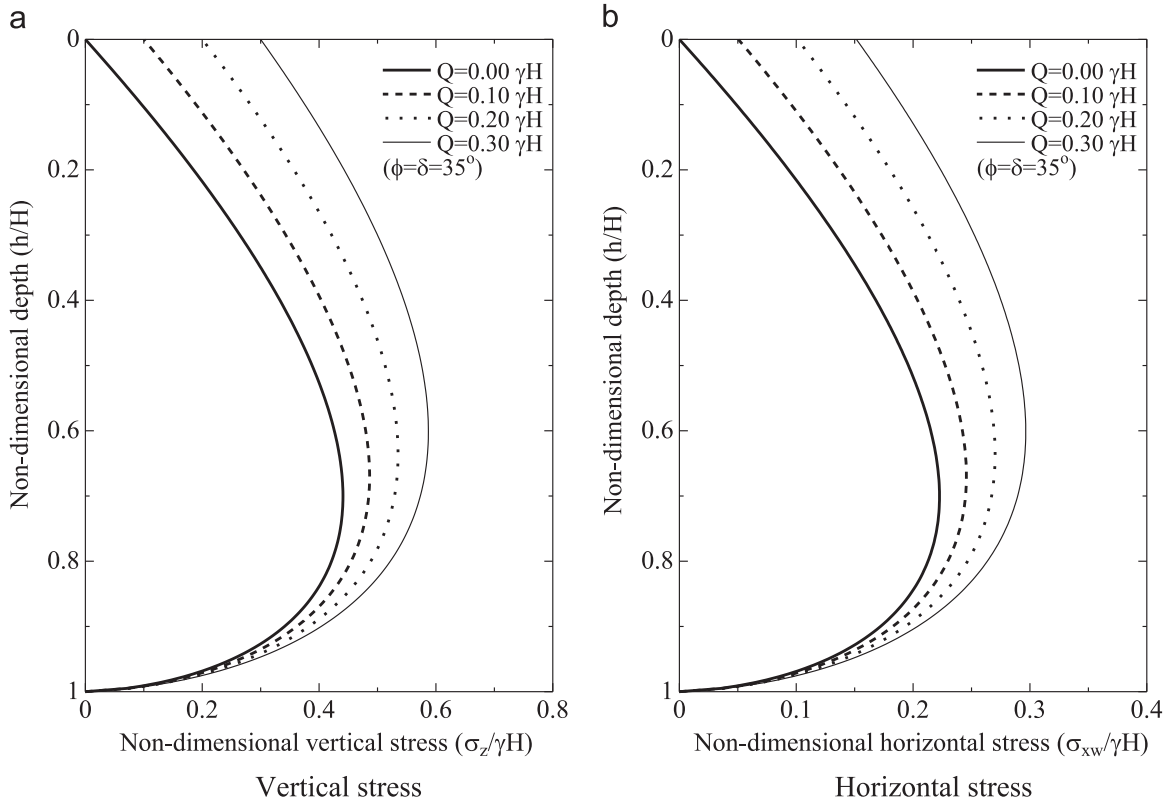

Fig. 8. Change in vertical and horizontal stresses at the wall with a change in uniform surcharge on the backfill soil.

stress:

$$\sigma_z(z)\Big|_{z=H}=0,\ \tau_{xz}(x,z)\Big|_{z=H}=0,\ \sigma_x(x,z)\Big|_{z=H}\geq 0 \qquad (19)$$

A similar discussion is reported in Rahmoun et al. (2009) and Pipatpongsa and Heng (2010) for stress field solutions in silos that the stress field solution theoretically corrects but unrealistic condition is inferred from the assumption of a uniformly distributed σ_z across a horizontal plane.

4. Illustration of stresses in the failure wedge

The illustrative stress solutions normalized by γH obtained from the proposed equations using $\phi=\delta=35^\circ$, $\mu_w=\tan\delta$ as retained soil properties with zero surcharge ($Q=0$) and wall height $H=1$ m are shown in Fig. 3 deduced from the proposed analysis.

Magnitude and direction of principal stresses in the failure wedge for the same retaining wall is illustrated in Fig. 4. It is clear in this figure that on the slip line, the principal directions coincide with vertical and horizontal directions. According to Fig. 4, when getting closer to the wall, principal stresses will rotate and reach their maximum rotation at the wall. Therefore shear stress (τ_{xz}) reaches its maximum magnitude at the wall (see Fig. 3).

Though a physical model set-up was developed and a series of experimental tests were conducted for this study, stress measurement was restricted to the wall surface due to the technical limitation of pressure gauge installation. In addition, the numerical solutions given by Loukidis and Salgado (2011) indicated that apart from the wall's face and the sliding face of the wedge, there is no shear band developing inside the sliding wedge when the wall movement is a pure translation. This is, therefore, consistent with the proposed stress distribution.

Unfortunately, the stress distribution obtained using the proposed method is shown without direct validation with experimental solutions or numerical solutions. Therefore, further comparisons are recommended in subsequent research.

5. Stresses at the wall

5.1. Stress distribution at the wall

The distribution of vertical, horizontal and shear stresses at the wall ($x=0$) is shown in Fig. 5, where the parameter $h=H-z$ in this figure represents a given height measured from the top of the wall. The stress profile along the wall is normalized by γH and H to the depth, respectively. It is obvious from this figure that the proposed analysis indicates the arching effect behind the retaining wall, because the maximum stresses do not appear at the toe, but at some distance away from the toe.

5.2. Influence of soil internal friction angle

The variation of the horizontal active earth pressure along the depth of the retaining wall obtained from the proposed formulations as a function of the backfill soil internal friction angle (ϕ) is shown in Fig. 6. It can be seen from this figure that as the internal friction angle increases from $\phi=0$, the distribution of the horizontal earth pressure changes from triangular to non-linear. Furthermore, as the internal friction angle increases, the horizontal earth pressure decreases and the height of the centroid of the lateral active earth pressure distribution increases.

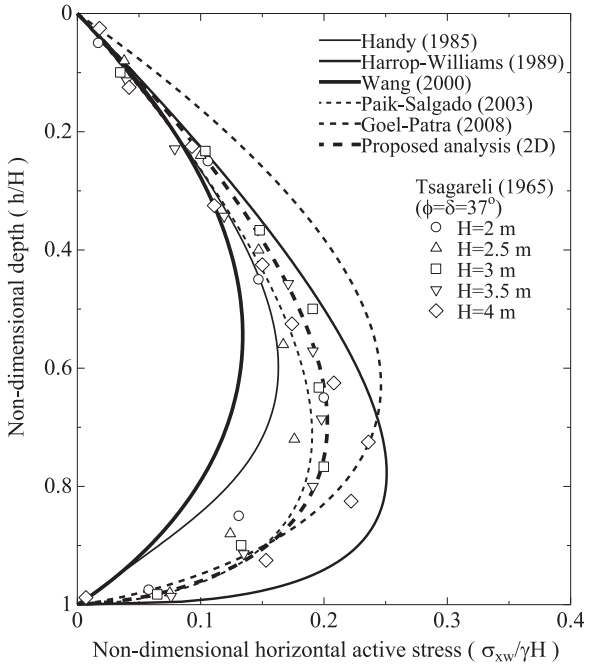

Fig. 9. Theoretical predictions for the distributions of horizontal active stress compared with full-scale measurements reported by Tsagareli (1965).

5.3. Influence of soil-wall interface friction angle

The variation of the horizontal active earth pressure along the retaining wall as a function of the soil-wall interface friction angle (δ) is shown in Fig. 7. The distribution of the lateral active earth pressure for $\delta=0$ is triangular as shown in this figure, consistent with Rankine's theory, and by increasing the interface friction changes to non-linear. It can also be seen from this figure that as the interface friction increases, the active pressure in the lower zone of the wall decreases and the height of the centroid of the lateral active earth pressure distribution increases.

5.4. Influence of surcharge

The variations in the active vertical and horizontal stress with a change in uniform surcharge are shown in Fig. 8. By increasing the magnitude of the surcharge Q, an increment in the vertical earth pressure in the upper zone of the wall can be observed, while the pressure decreases to zero at the base of the wall. Furthermore, it can be seen that the height of the centroid of the horizontal active force at the wall increases with increasing surcharge on the backfill soil.

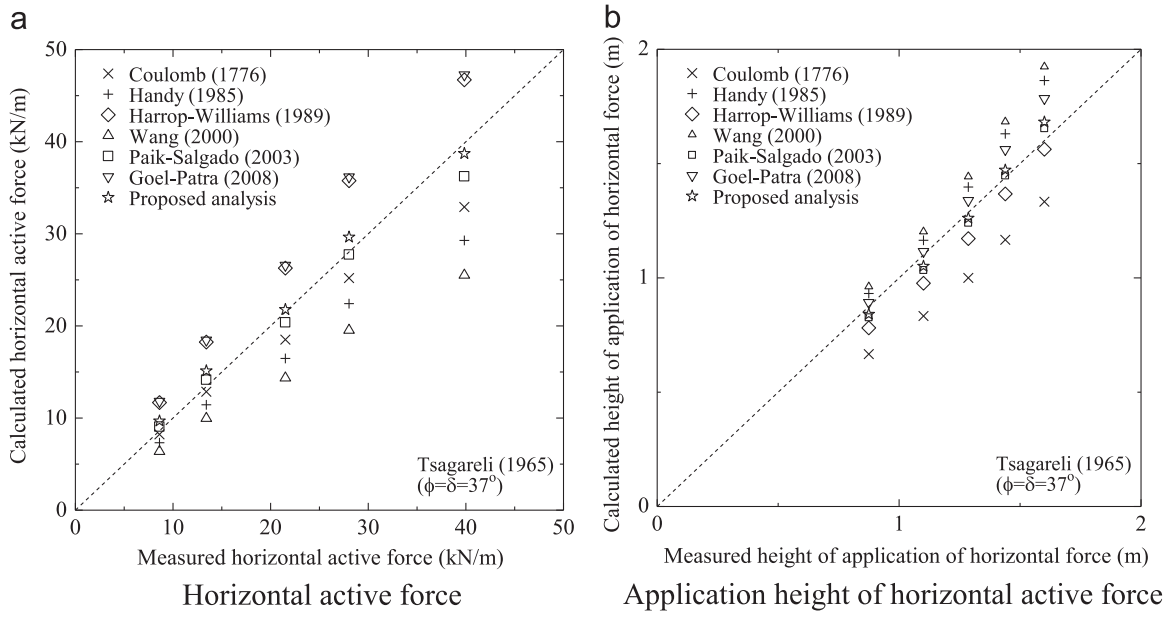

Fig. 10. Theoretical predictions compared with full-scale measurements reported by Tsagareli (1965).

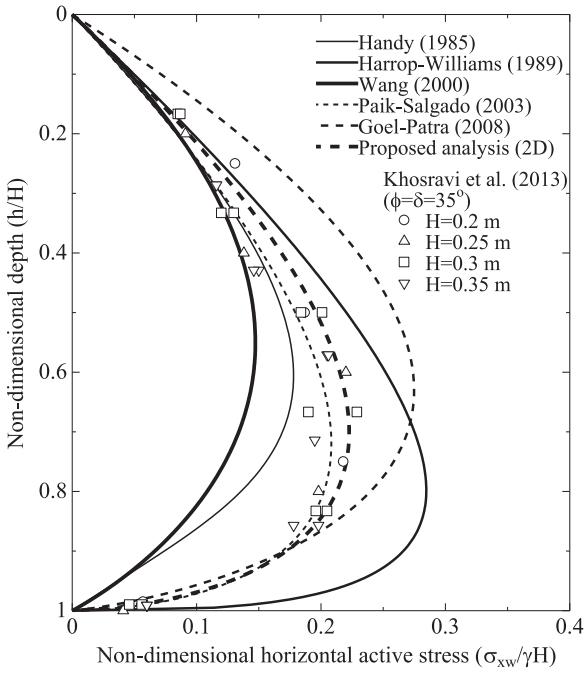

Fig. 11. Theoretical predictions for the distributions of horizontal active stress compared with laboratory-scale measurements reported by Khosravi et al. (2013).

5.5. Magnitude and height of application of horizontal active force

The horizontal active force (P_{ah}) on the rigid retaining wall can be obtained by integrating the equations of horizontal stress with respect to z at the wall where $x=0$:

$$P_{ah} = \int_0^H \sigma_x(x,z)\Big|_{x=0} dz. \tag{20}$$

Substituting Eq. (18) into Eq. (20) obtain the rigorous expressions of P_{ah} as shown in Eq. (21):

$$P_{ah} = \frac{K_w \gamma H^2}{1+n}\left(\frac{1}{2}+\frac{Q}{\gamma H}\right) \tag{21}$$

For the type of retaining wall whose back is vertical, the total active force on the wall (P_a) can be calculated from the addition of the horizontal active force normal to the wall (P_{ah}) and the shearing force acting tangentially to the wall (T). P_a makes an angle δ with the normal to the wall and can be calculated as follows:

$$P_a = \sqrt{{P_{ah}}^2+T^2} = \sqrt{{P_{ah}}^2+{P_{ah}}^2\tan^2\delta} = \frac{P_{ah}}{\cos\ \delta} \tag{22}$$

The height of the point of application of the total active force on the retaining wall coincides with the point of application of the horizontal active force. Therefore, this height can be calculated by dividing the moment of the horizontal stress about the wall base by the horizontal active force. Herein, the moment of the horizontal stress about the wall base (M) can be obtained by integration, as follows:

$$M = \int_0^H \sigma_x(x,z)\Big|_{x=0} z dz. \tag{23}$$

By substituting Eq. (18) into Eq. (23), rigorous expressions of M are obtained, as shown in Eq. (24):

$$M = \frac{K_w \gamma H^3}{2+n}\left(\frac{1}{3}+\frac{Q}{\gamma H}\right) \tag{24}$$

Finally, the height of application of the horizontal active force (h_a) estimated by the proposed analysis can be obtained by dividing Eq. (24) by Eq. (21).

$$h_a = \frac{2}{3}\frac{1+n}{2+n}\frac{\gamma H+3Q}{\gamma H+2Q}H \tag{25}$$

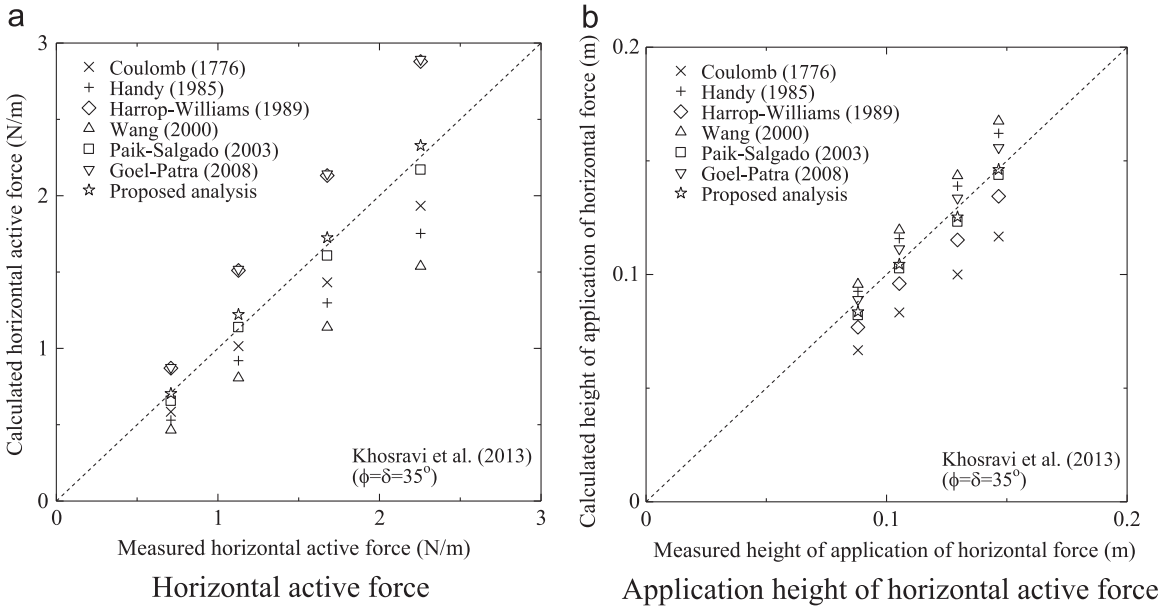

Fig. 12. Theoretical predictions compared with laboratory-scale measurements reported by Khosravi et al. (2013).

Table 1
Comparison of theoretical stress solutions' accuracy with the available experimental data via NRMSE (normalized root mean square error).

Theoretical solutions	Data of Tsagareli (1965)	Data of Khosravi et al. (2013)
Coulomb (1776)	0.41256	0.37531
Handy (1985)	0.16961	0.17222
Harrop-Williams (1989a)	0.18357	0.25015
Wang (2000)	0.21695	0.23063
Paik and Salgado (2003)	0.06569	0.05364
Goel and Patra (2008)	0.16520	0.22125
Proposed analysis (2D)	0.06566	0.06213

Because the arching effect is more prevalent for a wall with a rough surface, the smoother the surface of wall, the closer the profiles of horizontal stress at a retaining wall obtained from both analyses approaches to Rankine's active earth pressure. Therefore, for a frictionless wall surface ($\delta=0$) and the case of zero surcharge on the retained soil, $Q=0$, the height of application of the horizontal active force suggested by proposed analysis is one-third of the wall height, which is consistent with the results obtained from the Rankine theory.

6. Comparison with experimental results

In order to check the performance of the proposed analyses over various length scales, their predictions are compared with a series of full-scale model tests and also a series of laboratory-scale model tests with various wall heights in the following sub-sections. The results are also compared with the theoretical predictions from Handy (1985), Harrop-Williams (1989a), Wang (2000), Paik and Salgado (2003) and Goel and Patra (2008) where the failure line behind the wall is assumed to be linear and along the Coulomb slip surface in all of those methods.

6.1. Full-scale model tests

Some full-scale experimental results of Tsagareli (1965) are compared with the theoretical predictions from different methods developed based on the theory of arching effect in Fig. 9, where the soil properties are reported by Tsagareli (1965) as $\gamma=17.65$ kN/m^3 and $\phi=\delta=37^\circ$ for rough walls. It can be seen from this figure that the distribution of active earth pressures predicted by the proposed analysis is in good agreement with experimental data. The active horizontal stress profile for the proposed analysis is slightly higher than that of Paik and Salgado (2003).

A comparison of the magnitude and height of the point of application of the horizontal active force on the wall is shown in Fig. 10. From this figures it can be concluded that the proposed analysis provides the best predictions among the compared methods for the shown full-scale data. Because Coulomb's active wedge solution is generally expressed in terms of force, a linear pressure distribution with depth along a rough wall is assumed for calculating the application height of horizontal active force.

6.2. Laboratory-scale model tests

The proposed analysis is compared with the results of Khosravi et al. (2013) laboratory-scale model tests as shown in Figs. 11 and 12, where the unit weight of the backfill soil is 12.70 kN/m^3 and $\phi=\delta=35^\circ$. It can be seen that the proposed analysis predicted comparable results with both full-scale and laboratory-scale fully rough wall models. However, more investigations are necessary for actual designs of retaining walls since a fully rough condition is not commonly assumed in the actual design of a retaining wall.

With the aim of accuracy evaluation of each theoretical solution with the available experimental data, the normalized root mean square error (NRMSE) is employed to evaluate dimensionless residuals between predicted and observed values. Table 1 reports NRMSE of the predicted horizontal stresses at the wall by various solutions and the observed values reported by Tsagareli (1965) and Khosravi et al. (2013). By comparing with other solutions, the proposed solution as shown in Figs. 9–12 and Table 1 indicates that its prediction is as good as Paik and Salgado (2003).

The solution proposed in this study is generally under 2*D* formulation, giving the stress state not only on the retaining wall, but also in the failure zone between the wall and the slip plane. Moreover, this solution considered the existence of surcharge on the retained soil. When this stress field solution reduces to the stress distribution on the wall with no surcharge, there is no significant difference with the 1D solution proposed by Paik and Salgado (2003). On the other hand, this study demonstrates the significance of 2D formulation over 1D formulation by allowing the visualization of the trajectories of the principal stresses; therefore, soil arching action in the backfill can be depicted theoretically.

7. Conclusions

The problem of a rigid retaining wall with a uniform surcharge on the retained soil under active translation mode has been investigated in a two-dimensional system of equilibrium. Stress field solutions based on Janssen's assumptions were newly derived. These stress solutions were employed to calculate stress distribution at any arbitrary point in a failure wedge, including at the retaining wall and at the Coulomb slip line. The proposed analysis method indicates the arching effect behind the retaining wall because the maximum stresses did not appear at the toe, but at some distance away from the toe of the retaining wall. Because the arching effect is more prevalent for a wall with a rough surface, the smoother the surface of wall, the closer the profiles of horizontal stress at a retaining wall obtained from the proposed analyses to Rankine's active earth pressure.

In order to evaluate the applicability of the developed formulation, predictions based on the proposed solution were compared with both full-scale and laboratory-scale test results and estimation values given by existing equations. The predictions from the proposed analysis provided comparable approximations for the magnitude and height of the point of application of the horizontal active force among the compared analyses. It is acknowledged that the non-zero horizontal stress at the top of the retained soil was a drawback of this analysis. This can be attributed to the fact that the yield condition is not used in Janssen's approach and is slightly violated in the proposed analysis for stress states near the top surface.

Acknowledgment

This work was supported by KAKENHI (23760441 and 25820213) under Grants-in-Aid for Scientific Research from the Japan Society for the Promotion of Science. The first author acknowledges financial support from the Global COE Program, Center for Urban Earthquake Engineering (CUEE), Tokyo Institute of Technology.

References

Chang, M.F., 1997. Lateral earth pressures behind rotating walls. Can. Geotech. J. 34 (4), 498–509.
Chupin, O., Rechenmacher, A.L., Abedi, S., 2012. Finite strain analysis of non uniform deformation inside shear bands in sands. Int. J. Numer. Anal. Methods Geomech. 36 (14), 1651–1666.
Coulomb, C.A., 1776. Essai sur une application des règles de maximis & minimis à quelques problèmes de statique, relatifs à l'architecture. Mémoires De. Mathématique Et. De. Phys. De. l'Académie 7, 343–382.
Drescher, A., 1991. Analytical Methods in Bin-Load Analysis. Elsevier Science Ltd., Amsterdam.
Fang, Y., Ishibashi, I., 1986. Static earth pressures with various wall movements. J. Geotech. Eng. - ASCE 112 3, 317–333.
Getzler, Z., Komornik, A., Mazurik, A., 1968. Model study on arching above buried structures. J. Soil. Mech. Found. Div. - ASCE 94 SM5 (1123-1114).
Goel, S., Patra, N.R., 2008. Effect of Arching on Active Earth Pressure for Rigid Retaining Walls Considering Translation Mode. Int. J. Geomech. 8 (2), 123–133.
Guo, P., 2012. Critical length of force chains and shear band thickness in dense granular materials. Acta Geotech. 7 (1), 41–55.
Guo, P., Zhou, S., 2013. Arch in granular materials as a free surface problem. Int. J. Numer. Anal. Methods Geomech. 37 (9), 1048–1065.
Handy, R.L., 1985. The arch in soil arching. J. Geotech. Eng. - ASCE 111 (3), 302–318.
Handy, R., Spangler, M., 2007. Geotechnical Engineering: Soil and Foundation Principles and Practice. McGraw-Hill.
Harrop-Williams, K., 1989a. Arch in soil arching. J. Geotech. Eng. - ASCE 115 (3), 415–419.
Harrop-Williams, K., 1989b. Geostatic wall pressures. J. Geotech. Eng. - ASCE 115 (9), 1321–1325.
Iskander, M., Chen, Z., Omidbar, M., Guzman, I., Elsherif, O., 2013. Active static and seismic earth pressure for c-ϕ soils. Soils Found. 53 (5), 639–652.
Jáky, J., 1948. Earth pressure in silos, Proceedings of the 2nd International Conference on Soil Mechanics and Foundation Engineering. ICSMFE 1, 103–107.
Janssen, H.A., 1895. Versuche über Getreidedruck in Silozellen (Texts on grain pressure in silos), Zeitschr. d. Vereines Dtsch. Ingenieure 39, 1045–1049.
Khosravi, M.H., Pipatpongsa, T., Takemura, J., 2013. Experimental analysis of earth pressure against rigid retaining walls under translation mode. Géotechnique 63 (12), 1020–1028.
Krynine, D.P., 1945. Discussion of "Stability and stiffness of cellular cofferdams". Trans. Am. Soc. Civil. Eng. 10 (1), 1175–1178.
Loukidis, D., Salgado, R., 2011. Active pressure on gravity walls supporting purely frictional soils. Can. Geotech. J. 49 (1), 78–97.
Marston, A., Anderson, A.O., 1913. The theory of loads on pipes in ditches and tests of cement and clay drain tile and sewer pipe. Bull. Eng. Exp. Station 31, 1–181.
Millet, O., Rahmoun, J., de Saxcé, G., 2006. Analytic calculation of the stresses in an ensiled granular medium. C.r. Mec. 334 (2), 137–142.
Nadukuru, S., Michalowski, R., 2012. Arching in distribution of active load on retaining walls. J. Geotech. Geoenviron. Eng. 138 (5), 575–584.
O'Neal, T.S., Hagerty, D.J., 2011. Earth pressures in confined cohesionless backfill against tall rigid walls — a case history. Can. Geotech. J. 48 (8), 1188–1197.
Paik, K.H., Salgado, R., 2003. Estimation of active earth pressure against rigid retaining walls considering arching effects. Geotechnique 53 (7), 643–653.
Pipatpongsa, T., Heng, S., 2010. Granular arch shapes in storage silo determined by quasi-static analysis under uniform vertical pressure. J. Solid Mech. Mater. Eng. 4 8, 1237–1248.

Rahmoun, J., Millet, O., Saxce, Gd, 2008. A continuous media approach to modeling the stress saturation effect in granular silos. J. Stat. Mech.: Theory Exp. 2008 6, P06011–P06020.

Rahmoun, J., Millet, O., Fortin, J., 2009. Friction effect on stresses in ensiled granular media. Comput. Geotech. 36 (7), 1113–1124.

Rankine, W.J.M., 1857. On the stability of loose earth. Philos. Trans. R. Soc. Lond. 147, 9–27.

Rechenmacher, A., Abedi, S., Chupin, O., Orlando, A., 2011. Characterization of mesoscale instabilities in localized granular shear using digital image correlation. Acta Geotech. 6 (4), 205–217.

Saul, R.A., 1953. Measurements of grain pressures on bin walls and floors. Agric. Eng. 34, 231–234.

Sherif, M.A., Fang, Y., 1984. Dynamic earth pressures on walls rotating about the top. Soils Found. 24 (4), 109–117.

Sperl, M., 2006. Experiments on corn pressure in silo cells – translation and comment of Janssen's paper from 1895. Granul. Matter 8 (2), 59–65.

Take, W.A., Valsangkar, A.J., 2001. Earth pressures on unyielding retaining walls of narrow backfill width. Can. Geotech. J. 38 (6), 1220–1230.

Thay, S., Kitakata, S., Pipatpongsa, T., Takahashi, A., 2012. Measurements of vertical pressure profile beneath a planar valley of loose sand and its estimation based on self-similar solution of elliptic equation system. J. Jpn. Soc. Civil. Eng. Ser. A2 (Appl. Mech.) 68 (2), I21–I32.

Terzaghi, K., 1943. Theoretical Soil Mechanics. John Wiley and Sons.

Tsagareli, Z.V., 1965. Experimental investigation of the pressure of a loose medium on retaining walls with a vertical back face and horizontal backfill surface. Soil. Mech. Found. Eng. 2 (4), 197–200.

Walker, D.M., 1966. An approximate theory for pressures and arching in hoppers. Chem. Eng. Sci. 21 (11), 975–997.

Walters, J.K., 1973. A theoretical analysis of stresses in axially-symmetric hoppers and bunkers. Chem. Eng. Sci. 28 (3), 779–789.

Wang, W.L., Yen, B.C., 1974. Soil arching in slopes. J. Geotech. Eng. Div. - ASCE 100 (GT1), 61–78.

Wang, Y.Z., 2000. Distribution of earth pressure on a retaining wall. Geotechnique 50 (1), 83–88.